**ARTICLE**    OPEN

Check for updates

# Diffusion imaging genomics provides novel insight into early mechanisms of cerebral small vessel disease

Quentin Le Grand [1,2], Ami Tsuchida [1,3,4,5], Alexandra Koch [2], Mohammed-Aslam Imtiaz [2], N. Ahmad Aziz [2,6], Chloé Vigneron[1], Laure Zago[3,4,5], Mark Lathrop[7], Alexandre Dubrac[8,9,10], Thierry Couffinhal[11], Fabrice Crivello [3,4,5], Paul M. Matthews [12], Aniket Mishra [1], Monique M. B. Breteler [2,13], Christophe Tzourio [1,14] and Stéphanie Debette [1,15 ✉]

Cerebral small vessel disease (cSVD) is a leading cause of stroke and dementia. Genetic risk loci for white matter hyperintensities (WMH), the most common MRI-marker of cSVD in older age, were recently shown to be significantly associated with white matter (WM) microstructure on diffusion tensor imaging (signal-based) in young adults. To provide new insights into these early changes in WM microstructure and their relation with cSVD, we sought to explore the genetic underpinnings of cutting-edge tissue-based diffusion imaging markers across the adult lifespan. We conducted a genome-wide association study of neurite orientation dispersion and density imaging (NODDI) markers in young adults (i-Share study: $N = 1\,758$, (mean[range]) 22.1[18–35] years), with follow-up in young middle-aged (Rhineland Study: $N = 714$, 35.2[30–40] years) and late middle-aged to older individuals (UK Biobank: $N = 33\,224$, 64.3[45–82] years). We identified 21 loci associated with NODDI markers across brain regions in young adults. The most robust association, replicated in both follow-up cohorts, was with Neurite Density Index (NDI) at chr5q14.3, a known WMH locus in *VCAN*. Two additional loci were replicated in UK Biobank, at chr17q21.2 with NDI, and chr19q13.12 with Orientation Dispersion Index (ODI). Transcriptome-wide association studies showed associations of *STAT3* expression in arterial and adipose tissue (chr17q21.2) with NDI, and of several genes at chr19q13.12 with ODI. Genetic susceptibility to larger WMH volume, but not to vascular risk factors, was significantly associated with decreased NDI in young adults, especially in regions known to harbor WMH in older age. Individually, seven of 25 known WMH risk loci were associated with NDI in young adults. In conclusion, we identified multiple novel genetic risk loci associated with NODDI markers, particularly NDI, in early adulthood. These point to possible early-life mechanisms underlying cSVD and to processes involving remyelination, neurodevelopment and neurodegeneration, with a potential for novel approaches to prevention.

*Molecular Psychiatry*; https://doi.org/10.1038/s41380-024-02604-7

## INTRODUCTION

Cerebral small vessel disease (cSVD) is a leading cause of stroke and cognitive decline, and likely the main pathological substrate underlying the vascular contribution to dementia [1]. It is also a common cause of gait, balance, and mood disorders in older persons [2]. This condition is most often covert, i.e. detectable on brain imaging in individuals with no apparent neurological history. MRI-markers of cSVD are extremely common in the general population with increasing age, with a prevalence and burden rising more drastically after age 65 [3]. Extensive covert cSVD was shown in numerous longitudinal studies to portend a two- to three-fold increased risk of stroke and dementia [4, 5]. White matter hyperintensities (WMH), the most common neuroimaging feature of cSVD, was shown to be associated with an increased risk of Alzheimer disease, with evidence for a causal relation using Mendelian randomization [4, 6, 7]. Thus covert cSVD should be a major target to prevent stroke and dementia in the population, an opportunity that has been largely neglected to date. While optimal management of vascular risk factors, especially hypertension, was shown to slow down the progression of cSVD [8], an important limitation is the lack of mechanism-based drugs, targeting the disease process underlying cSVD. Identifying novel therapeutic targets requires better understanding of molecular pathways involved.

[1]University of Bordeaux, INSERM, Bordeaux Population Health research center, UMR1219, F-33000 Bordeaux, France. [2]Population Health Sciences, German Center for Neurodegenerative Diseases (DZNE), Bonn, Germany. [3]University of Bordeaux, Institute of Neurodegenerative Diseases, UMR5293, Neurofunctional Imaging Group, F-33000 Bordeaux, France. [4]CNRS, Institute of Neurodegenerative Diseases, UMR5293, Neurofunctional Imaging Group, F-33000 Bordeaux, France. [5]CEA, Institute of Neurodegenerative Diseases, UMR5293, Neurofunctional Imaging Group, F-33000 Bordeaux, France. [6]Department of Neurology, Faculty of Medicine, University of Bonn, Bonn, Germany. [7]Department of Human Genetics, McGill University, Montreal, Quebec, Canada; Victor Phillip Dahdaleh Institute of Genomic Medicine at McGill University, Montreal, QC H3A 0G1, Canada. [8]Centre de Recherche, CHU Sainte-Justine, Montréal, QC, Canada. [9]Département de Pathologie et Biologie Cellulaire, Université de Montréal, Montréal, QC, Canada. [10]Département d'Ophtalmologie, Université de Montréal, Montréal, QC, Canada. [11]University of Bordeaux, INSERM, Biologie des maladies cardiovasculaires, U1034, F-33600 Pessac, France. [12]UK Dementia Research Institute and Department of Brain Sciences, Imperial College, London, UK. [13]Institute for Medical Biometry, Informatics and Epidemiology (IMBIE), Faculty of Medicine, University of Bonn, Bonn, Germany. [14]Bordeaux University Hospital, Department of Medical Informatics, F-33000 Bordeaux, France. [15]Bordeaux University Hospital, Department of Neurology, Institute for Neurodegenerative Diseases, F-33000 Bordeaux, France. ✉email: stephanie.debette@u-bordeaux.fr

Genome-wide association studies (GWAS) are a powerful tool to unravel molecular mechanisms underlying complex diseases. In recent years they identified numerous common genetic variants associated with MRI-markers of cSVD, such as WMH volume [6, 9, 10]. Intriguingly, we recently showed that genetic risk variants for WMH volume identified in older persons are associated with changes in white matter microstructure on diffusion tensor imaging (DTI) already at age 20, in a direction compatible with changes shown to precede the occurrence of WMH in older age (reduced fractional anisotropy and increased mean diffusivity and peak width of skeletonized mean diffusivity) [6, 11, 12]. This suggests that processes contributing to cSVD may find their root much earlier in life than previously thought [6, 13, 14], also dovetailing with emerging evidence that late-life neurodegenerative disorders have early-life and neurodevelopmental determinants amenable to treatment [15, 16].

In contrast with "traditional" MRI-markers of cSVD, such as WMH, lacunes, or cerebral microbleeds, reflecting advanced tissue damage and detectable mostly in late middle to older age, markers of white matter microstructure based on diffusion MRI (dMRI) may capture changes predisposing to cSVD much earlier in life. This could be useful for unraveling molecular mechanisms leading to cSVD throughout the life course, with possible implications for prevention and treatment much earlier in the disease process. DTI, the most commonly used type of dMRI, measures variations in magnitude or directionality of diffusivity but cannot distinguish underlying biological processes (signal-based) [17–19]. More recently, novel biophysical, tissue-based diffusion models derived from multi-shell acquisitions have been developed, such as neurite orientation dispersion and density imaging (NODDI) to provide better descriptions of the underlying tissue properties [17, 20]. NODDI metrics include proxies for the density of neurites (Neurite Density Index, NDI) relative to extra-neurite volume (such as extracellular matrices, microglia and astrocytes), the dispersion of neurite orientation (Orientation Dispersion Index, ODI), and proportion of free water (Isotropic Volume Fraction, ISOVF), i.e. CSF [20, 21].

A recent GWAS in older UK Biobank participants (mean age 64.3 years) [22] identified numerous loci associated with regional NODDI markers. However, to our knowledge, genetic determinants of NODDI markers in younger age groups are unknown. Here we sought to identify loci associated with NODDI markers of white matter microstructure specifically in young adults, when brain white matter maturation peaks. We were then interested in exploring the relation of identified NODDI loci with cSVD, as well as other later onset neurological diseases, given the aforementioned evidence on the role of early life factors. Moreover, we explored how vascular risk factors, which are crucial determinants of cSVD and brain health at large, may already impact white matter microstructure in early adulthood.

## MATERIALS AND METHODS
### Study population
To explore the genetic determinants of NODDI markers in young adults we used the Internet-based Students HeAlth Research Enterprise (i-Share) study, a prospective population-based cohort study of French-speaking students [23]. Here we used the sub-sample of 1758 participants aged 18–35 years for whom both brain MRI and genome-wide genotype data were available, through the MRi-Share and bio-Share ancillary studies (mean age ± standard deviation (SD): 22.1 ± 2.3 years; 72.2% women) [19, 24, 25].

For follow-up in young middle-aged adults of genetic associations observed in i-Share, we used the Rhineland Study, an ongoing community-based prospective cohort study that invites inhabitants aged 30 years and above living in the city of Bonn, Germany, to participate [26]. We used baseline data of a sub-sample of 714 Rhineland Study participants aged 30–40 years with both genotype data and MRI scans available, and no neurological disorder (mean age ± SD: 35.2 ± 3.1 years; 54% women).

Detailed information on both cohorts is presented in the Supplementary methods.

For follow-up in late middle-aged to older adults of genetic associations observed in i-Share, we used summary statistics from the latest published GWAS on NODDI markers in the UK Biobank ($N = 33,224$, 52.4% women, mean age: 64.3 [range, 45.1–81.8] years) [22].

All human research presented in this manuscript was approved by relevant ethics committees and/or institutions and was conducted according to the Declaration of Helsinki. All participants provided written informed consent.

### MRI acquisition and phenotyping
Similar scanners (3-Tesla Siemens Prisma for the i-Share and Rhineland studies and 3-Tesla Siemens Skyra for UK Biobank) and similar diffusion MRI protocols were used for the three cohorts, described in the Supplementary methods and in detail elsewhere [19, 22, 24, 26–29]. To generate regional NODDI phenotypes, all cohorts used the standard tract-based spatial statistics (TBSS) framework and the JHU ICBM DTI-81 atlas [20, 22, 26, 27, 29–37]. This atlas is a stereotaxic probabilistic white matter atlas that fuses DTI-based white matter information with an anatomical template (ICBM-152). The derived white matter parcellation map enables to define 27 white matter anatomic structures segmented based on fiber orientation information (Table S1). In the i-Share and Rhineland studies, we also generated one global measure across the full white matter, in addition to the 27 regional markers (Table S1) for each of the three NODDI metrics (NDI, ODI, ISOVF), leading to 84 NODDI markers in total (Supplementary methods). To normalize distributions we applied a rank-based inverse normal transformation to the 84 variables in both cohorts. For UK Biobank, we derived data for the three NODDI metrics in the same 27 regions, for 21 of which GWAS summary statistics of lateralized values only (left and right) were provided, leading to 144 NODDI markers (no global measure was available) [22, 27, 28].

### Genotyping, quality control, and imputation
Genome-wide genotyping was performed using the Affymetrix Precision Medicine Axiom Array for i-Share, Affymetrix UK BiLEVE Axiom Array and UK Biobank Axiom Array for UK Biobank, and the Infinium Omni2.5Exome-8 BeadChip for Rhineland. Genotypes were imputed to the Haplotype Reference Consortium (HRC, i-Share, UK Biobank) and 1000 Genomes p3v5 (Rhineland Study) reference panels. Quality control procedures were described in the Supplementary methods and in detail elsewhere [25, 38, 39].

### Statistical analyses
Analytical steps are summarized in Fig. 1.

### GWAS
We performed 84 GWAS using genome-wide linear mixed models implemented in REGENIE v2.2 [40]. Analyses were restricted to Single Nucleotide Polymorphisms (SNPs) with an imputation score >0.5 and a minor allele frequency (MAF) > 0.01 and adjusted for age at MRI, sex (reported and concordant with genetically determined sex), total intracranial volume and the first four principal components of population stratification (details in Supplementary methods) [25].

Using matSPDlite in R to account for correlation between the 84 NODDI markers, we identified 39.45 independent markers, leading to a significance threshold of $p < 1.27 \times 10^{-9}$ [41]. We also considered as "suggestive" SNPs reaching genome-wide significance at $p < 5 \times 10^{-8}$.

In middle-aged adults of the Rhineland Study we followed up NODDI-associated loci identified in i-Share using the same linear mixed model, adjusting for age at MRI, sex, intracranial volume and the first ten principal components of population stratification [42]. When the lead SNP from the i-Share GWAS was not available, we used the best LD-proxy (LD-$r^2$ > 0.50). Next, to expand our results to older adults, we followed up NODDI-associated loci from i-Share in the latest NODDI GWAS from UK Biobank ($N = 33,224$) [22]. SNPs with p < $2.38 \times 10^{-3}$ (correcting for 21 independent loci) were considered replicated. We also performed sex-specific association analyses for genome-wide significant NODDI-associated SNPs in the three samples.

*Shared genetic variation of NODDI markers with neurological and vascular traits.* We explored the association of genome-wide significant NODDI loci identified in i-Share (lead SNPs and their LD-proxies in a 1 Mb
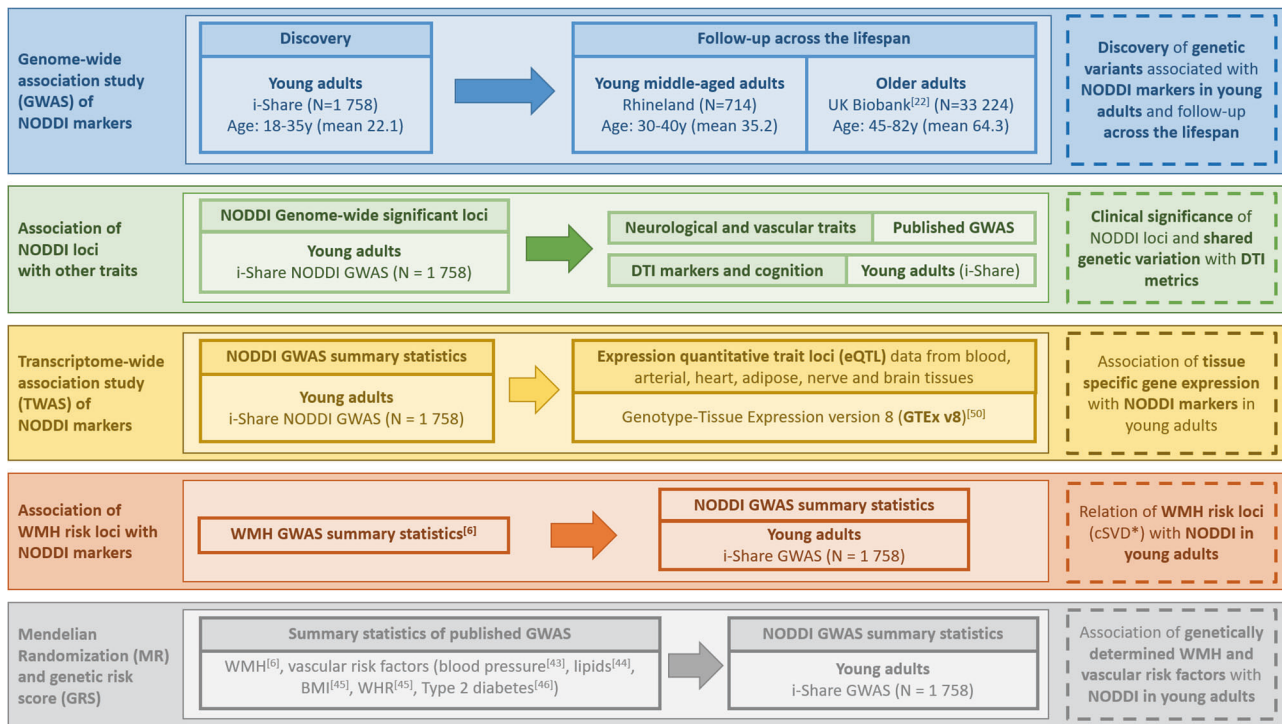
**Fig. 1 Study workflow.** * WMH risk loci reflect genetic susceptibility to cerebral small vessel disease (cSVD). BMI Body mass index, DTI Diffusion tensor imaging, NODDI Neurite orientation dispersion and density imaging, WHR Waist-to-hip ratio adjusted for BMI; WMH White matter hyperintensities.

window and with $r^2 > 0.9$) with several neurological and vascular traits, using the largest available European ancestry GWAS summary statistics thereof: blood pressure (systolic [SBP], diastolic blood pressure [DBP] and pulse pressure [PP], $N = 757,601$) [43], lipids (LDL-, HDL-cholesterol, triglycerides [TG], $N = 1,320,016$) [44], body mass index (BMI) ($N = 806,834$) [45], waist-to-hip ratio adjusted for BMI (WHR) ($N = 694,649$) [45], type 2 diabetes ($N = 74,124/824,006$) [46], WMH ($N = 50,970$) [6], Alzheimer disease ($N = 111,326/677,663$) [47], and multiple sclerosis (MS) ($N = 14,802/26,703$) [48]. Genetic associations with these traits at $p < 1.98 \times 10^{-4}$ (Bonferroni-corrected threshold for 21 loci and 12 traits) were considered statistically significant.

*Association of NODDI loci with cognitive performance and with diffusion tensor imaging markers in young adults.* To explore their clinical relevance in young adults, we examined the association of genome-wide significant NODDI loci identified in i-Share (lead SNPs) with scores of 8 cognitive tests in the same cohort (Supplementary methods). Associations were tested using similar regression models as for the NODDI GWAS, adjusting for age, sex, and the first four principal components of population stratification. Genetic associations at $p < 2.98 \times 10^{-4}$ (correcting for 21 loci and 8 traits) were considered significant. We further tested the association of NODDI loci with the two most studied DTI markers in i-Share, fractional anisotropy (FA) and mean diffusivity (MD), in the same regions of interest. Genetic associations at $p < 1.19 \times 10^{-3}$ (correcting for 21 loci and 2 traits) were considered significant.

*Transcriptome-wide association study on the genome-wide significant NODDI loci in young adults.* We performed transcriptome-wide association studies (TWAS) using TWAS-Fusion [49] to identify genes whose expression is significantly associated with NODDI markers. We focused on genome-wide significant, replicated NODDI GWAS loci. We used precomputed functional weights from publicly available gene expression reference panels (expression quantitative trait loci [eQTL]) from tissues considered relevant for cerebrovascular disease (blood, arterial, heart, adipose, nerve and brain tissues) and cross-tissue weights generated using sparse canonical correlation analysis (sCCA), from the Genotype-Tissue Expression version 8 (GTEx v8) [50, 51]. Transcriptome-wide significance at $p < 7.8 \times 10^{-6}$ was based on the average number of features (6400 genes) tested across tissues, and we also considered suggestive associations with

$p < 1 \times 10^{-4}$. These genes were then tested in conditional analyses in TWAS-Fusion [49]. Next, we performed a colocalization analysis (COLOC) on the conditionally significant genes ($p < 0.05$) to estimate the posterior probability of a shared causal variant between the gene expression and trait association (PP4) [52], considering genes with PP4 ≥ 0.75 as colocalized. Colocalized genes with eQTLs reaching genome-wide significance in association with the corresponding NODDI marker (or in moderate-high LD, $r^2 > 0.5$, with the lead SNP) were considered as being in a GWAS locus, others were considered as pointing to "novel" loci (Supplementary methods).

*Lifetime brain gene expression profile.* We examined the spatio-temporal expression pattern of genes in genome-wide significant NODDI loci identified in i-Share that also colocalized in the TWAS analyses. We used a public database (https://hbatlas.org/) comprising genome-wide exon-level transcriptome data from 1340 tissue samples from 16 brain regions of 57 postmortem human brains, from embryonic development to late adulthood [53].

*Association of WMH risk loci with NODDI markers in young adults.* We explored associations with NODDI markers in young adults of 25 known WMH risk loci previously identified in older European-ancestry populations [6]. We extracted association results of these 25 loci from the GWAS of global NDI, ODI and ISOVF in i-Share, using $p < 2 \times 10^{-3}$ as the significance threshold.

*Association of genetically determined WMH and vascular risk factors with NODDI markers in young adults.* To examine the association of genetically determined WMH and vascular risk factors with the NODDI markers in i-Share, we first generated weighted genetic risk scores (GRS) using independent ($r^2 > 0.01$) genome-wide significant variants ($p < 5 \times 10^{-8}$) from the largest European-ancestry GWAS summary statistics for blood pressure [43], lipids [44], BMI [45], WHR [45], type 2 diabetes [46], and WMH [6]. Associations were tested using linear mixed models adjusted for age, sex, total intracranial volume, and the first four principal components of population stratification (Supplementary methods). Results with $p < 1.27 \times 10^{-3}$ (accounting for 39.45 independent NODDI markers) were considered significant [41]. Next, for significant results in GRS analyses, we performed two-sample Mendelian randomization (MR) analyses to seek

**Table 1.** Genome-wide significant SNPs associated with NODDI markers in the i-Share cohort and replication in the Rhineland study and UK Biobank.

| Region of interest | SNP | Locus | Position | Nearest genes | Function | A0 | A1 | i-Share [18–35 yl (n = 1 758)] | | | | RLS [30–40 yl (n = 714)] | | | UKB [45–82 yl (n = 33 224)] | | |
|---|---|---|---|---|---|---|---|---|---|---|---|---|---|---|---|---|---|
| | | | | | | | | Freq | Beta | SE | p | Beta | SE | p | Beta | SE | p |
| **Global metrics** | | | | | | | | | | | | | | | | | |
| ISOVF | rs4889450 | 16q23.3 | 82041436 | SDR42E1 | Intronic | G | T | 0.09 | 0.32 | 0.06 | 2.80E-08 | | | | | | |
| **NDI** | rs10052710 | 5q14.3 | 82860025 | VCAN | Intronic | G | T | 0.80 | 0.23 | 0.04 | 2.32E-09 | **0.21** | **0.05** | **6.85E-05** | | | |
| ODI | rs9819179 | 3q13.31 | 115173615 | ZBTB20;GAP43 | Intergenic | A | G | 0.95 | 0.37 | 0.07 | 2.01E-08 | -0.08 | 0.09 | 3.53E-01 | | | |
| **Specific regions of interest** | | | | | | | | | | | | | | | | | |
| **ISOVF** | | | | | | | | | | | | | | | | | |
| Middle cerebellar peduncle | rs77827241 | 3q28 | 191973700 | FGF12-AS1 | ncRNA intronic | T | C | 0.04 | 0.47 | 0.08 | 2.09E-08 | | | | -0.02 | 0.02 | 4.16E-01 |
| Posterior corona radiata | rs2710548 | 4q28.1 | 126273530 | FAT4 | Intronic | C | T | 0.58 | 0.17 | 0.03 | 2.49E-08 | -0.08 | 0.04 | 5.62E-02 | -0.01 | 0.01 | 3.96E-01 |
| External capsule | rs3775205 | 4q34.3 | 177590724 | SPCS3;VEGFC | Intergenic | C | T | 0.20 | 0.21 | 0.04 | 4.33E-08 | 0.02 | 0.04 | 6.65E-01 | 0.00 | 0.01 | 7.32E-01 |
| Middle cerebellar peduncle | rs7971607 | 12q24.31 | 122330480 | PSMD9 | Intronic | A | G | 0.43 | 0.17 | 0.03 | 6.18E-09 | 0.04 | 0.04 | 3.36E-01 | 0.00 | 0.01 | 6.20E-01 |
| Cingulum cingulate gyrus | rs9904001 | 17q24.1 | 63309198 | RGS9;LINC02563 | Intergenic | G | A | 0.80 | 0.22 | 0.04 | 4.05E-09 | 0.04 | 0.05 | 4.81E-01 | 0.00 | 0.01 | 9.57E-01 |
| Uncinate fasciculus | rs8101200 | 19q13.31 | 44051558 | XRCC1 | Intronic | G | A | 0.12 | 0.28 | 0.05 | 1.04E-08 | 0.08 | 0.07 | 2.77E-01 | 0.03 | 0.01 | 7.30E-02 |
| **NDI** | | | | | | | | | | | | | | | | | |
| Retrolenticular part of the internal capsule | rs72642850 | 1p36.23 | 7526759 | CAMTA1 | Intronic | A | G | 0.16 | 0.21 | 0.04 | 3.27E-08 | 0.00 | 0.05 | 9.74E-01 | 0.01 | 0.01 | 4.27E-01 |
| **Posterior corona radiata** | rs13176921 | 5q14.3 | 82860348 | VCAN | Intronic | G | A | 0.79 | 0.22 | 0.04 | 4.67E-09 | **0.19** | **0.05** | **4.62E-04** | **0.16** | **0.01** | **2.94E-57** |
| **Posterior thalamic radiation** | rs13176921 | 5q14.3 | 82860348 | VCAN | Intronic | G | A | **0.79** | **0.27** | **0.04** | **4.50E-12** | **0.16** | **0.05** | **1.70E-03** | **0.18** | **0.01** | **6.68E-75** |
| **Superior longitudinal fasciculus** | rs13176921 | 5q14.3 | 82860348 | VCAN | Intronic | G | A | 0.79 | 0.22 | 0.04 | 4.59E-09 | **0.18** | **0.05** | **3.55E-04** | **0.16** | **0.01** | **1.66E-60** |
| **Sagittal stratum** | rs13176921 | 5q14.3 | 82860348 | VCAN | Intronic | G | A | 0.79 | 0.20 | 0.04 | 3.73E-08 | **0.16** | **0.05** | **1.84E-03** | **0.19** | **0.01** | **3.63E-84** |
| Posterior corona radiata | rs13257545 | 8q12.1 | 56531057 | XKR4;TMEM68 | Intergenic | A | G | 0.07 | 0.34 | 0.06 | 3.35E-08 | -0.04 | 0.09 | 6.17E-01 | -0.01 | 0.02 | 6.90E-01 |
| **Fornix cres or stria terminalis** | rs1053004 | 17q21.2 | 40466092 | STAT3 | UTR3 | A | G | **0.40** | **0.18** | **0.03** | **1.16E-09** | 0.02 | 0.04 | 6.00E-01 | **0.03** | **0.01** | **2.01E-03[b]** |
| Retrolenticular part of the internal capsule | rs1053004 | 17q21.2 | 40466092 | STAT3 | UTR3 | A | G | 0.40 | 0.17 | 0.03 | 4.71E-08 | 0.00 | 0.04 | 9.07E-01 | 0.02 | 0.01 | 5.05E-02 |
| **Sagittal stratum** | rs1053004 | 17q21.2 | 40466092 | STAT3 | UTR3 | A | G | 0.40 | 0.18 | 0.03 | 2.39E-08 | -0.02 | 0.04 | 6.32E-01 | **0.03** | **0.01** | **1.06E-03[b]** |
| Posterior corona radiata | rs17833531[a] | 18q22.2 | 68348916 | GTSCR1;LINC01541 | Intergenic | A | G | 0.92 | 0.33 | 0.06 | 2.80E-08 | 0.06 | 0.06 | 3.20E-01 | 0.01 | 0.01 | 5.15E-01 |
| **ODI** | | | | | | | | | | | | | | | | | |
| Anterior corona radiata | rs12126432 | 1p13.1 | 116595405 | SLC22A15 | Intronic | G | C | 0.97 | 0.60 | 0.11 | 3.12E-08 | 0.09 | 0.10 | 3.49E-01 | 0.02 | 0.02 | 3.00E-01 |
| Cingulum cingulate gyrus | rs4920174 | 1q42.2 | 234054627 | SLC35F3 | Intronic | T | C | 0.98 | 0.86 | 0.15 | 1.20E-08 | | | | | | |
| Superior fronto-occipital fasciculus | rs10516765 | 4q21.23 | 86847135 | ARHGAP24 | Intronic | A | G | 0.99 | 0.91 | 0.15 | 3.70E-09 | | | | | | |

**Table 1.** continued

| Region of interest | SNP | Locus | Position | Nearest genes | Function | A0 | A1 | i-Share [18–35 yl] (n = 1 758) | | | | RLS [30–40 yl] (n = 714) | | | UKB [45–82 yl] (n = 33 224) | | |
|---|---|---|---|---|---|---|---|---|---|---|---|---|---|---|---|---|---|
| | | | | | | | | Freq | Beta | SE | p | Beta | SE | p | Beta | SE | p |
| Sagittal stratum | rs11185683[a] | 9q34.2 | 137131455 | RNU6ATAC/LINC02247 | Intergenic | A | G | 0.96 | 0.54 | 0.09 | 1.43E-08 | -0.04 | 0.13 | 7.72E-01 | 0.01 | 0.02 | 5.39E-01 |
| Anterior corona radiata | rs4968557 | 17q23.2 | 59462087 | BCAS3 | Intronic | A | G | 0.87 | 0.29 | 0.05 | 2.96E-08 | 0.02 | 0.08 | 7.73E-01 | -0.01 | 0.02 | 7.22E-01 |
| **Medial lemniscus** | **rs807478[a]** | **19q13.12** | **36252494** | **PROSER3** | **Intronic** | **G** | **A** | **0.49** | **0.15** | **0.03** | **3.12E-08** | **0.05** | **0.04** | **2.41E-01** | **0.03** | **0.01** | **3.05E-05** |
| Cingulum cingulate gyrus | rs56083857 | 22q11.23 | 25386309 | TMEM211/KIAA1671 | Intergenic | T | C | 0.89 | 0.31 | 0.05 | 3.76E-09 | -0.09 | 0.07 | 1.84E-01 | 0.01 | 0.01 | 5.68E-01 |
| Body corpus callosum | rs77240077 | 22q12.1 | 26944635 | TPST2 | Intronic | G | A | 0.05 | 0.38 | 0.07 | 3.94E-08 | 0.15 | 0.10 | 1.46E-01 | -0.03 | 0.02 | 1.41E-01 |

$P < 1.27 \times 10^{-9}$ for the i-Share study and $p < 2.38 \times 10^{-3}$ for UK Biobank and Rhineland Study are in bold.

*RLS* Rhineland Study, *UKB* UK Biobank [22], *A1* effect allele, *A0* non-effect allele, *Freq* frequency of A1 in the i-Share study, *Beta* effect for A1 in the i-Share study, *SE* Standard error, *NDI* Neurite Density Index, *ODI* Orientation Dispersion Index, *ISOVF* Isotropic Volume Fraction.

[a]rs17833531, rs807478 and rs11185683 were not available in the Rhineland study, results are presented for their proxies rs80237634 (LD-$r^2 = 0.58$), rs173003 (LD-$r^2 = 0.98$) and rs11185685 (LD-$r^2 = 0.99$) in this study.

[b]Significant only for left region of interest. For UK Biobank results, the results are presented for the most significant laterality (Left/Right) for lateralized metrics.

evidence for a causal relation of WMH and vascular risk factors with NODDI markers (Supplementary methods). To build genetic instruments we used independent ($r^2 > 0.01$) genome-wide significant ($p < 5 \times 10^{-8}$) risk variants as in GRS analyses. We used three distinct two-sample MR approaches to strengthen the validity of our findings: RadialMR [54], Generalised Summary-data-based Mendelian Randomisation (GSMR) [55] and Two-SampleMR [56]. We considered RadialMR after outlier removal and GSMR as primary analyses. In addition to classical inverse-variance weighted (IVW) analyses, we applied MR methods that are more robust to the use of pleiotropic instruments (weighted median, MR-Egger, analyses excluding instruments showing heterogeneity). Given the relatively small sample for MR analyses, we used a significance threshold of $p < 0.05$, in an exploratory setting.

Finally, we examined whether brain regions where genetically determined WMH was associated with NODDI markers in young adults overlap with regions most frequently harboring WMH in older adults. We projected (on axial multi-slices) WMH GRS Z-scores for significant associations with NDI in i-Share onto the corresponding white matter regions, overlaying this projection with the frequency of WMH occurrence across white matter regions in older adults participating in the population-based 3C-Dijon study ($N = 1781$, mean age: 72.4[65–85] years) [57, 58]. We computed the mean WMH frequency for 3C-Dijon participants in each of the 27 JHU regions to test their correlation with Z-scores of association between the WMH GRS and NDI within each JHU region in the i-Share cohort.

## RESULTS
### Genetic susceptibility to tissue-based variations of white matter microstructure in young adults
Using GWAS for 84 NODDI markers in 1 758 young adults from the i-Share study (mean age 22.1), we identified 27 genome-wide significant associations ($p < 5 \times 10^{-8}$) in 21 genomic loci (Table 1, Fig. 2, Figs. S1–2). Two of these remained significant after additionally correcting for the number of independent NODDI markers tested ($p < 1.27 \times 10^{-9}$), at chr5q14.3 in *VCAN*, associated with NDI in the posterior thalamic radiation (PTR, $p = 4.50 \times 10^{-12}$), and at chr17q21.2 in *STAT3*, associated with NDI in the fornix cres or stria terminalis (FX.ST, $p = 1.16 \times 10^{-9}$). The chr5q14.3 locus was associated with NDI at $p < 5 \times 10^{-8}$ in several other regions besides PTR, i.e. the posterior corona radiata (PCR), superior longitudinal fasciculus (SLF) and sagittal stratum (SS), and with global NDI. Associations with NDI markers at chr5q14.3 replicated ($p < 2.38 \times 10^{-3}$) both in the Rhineland Study and UK Biobank (mean age 35.2 and 64.3 years), even reaching genome-wide significance in the latter. Two additional genome-wide significant loci identified in i-Share replicated in the UK Biobank, at chr17q21.2 (*STAT3*) for NDI-FX.ST and NDI-SS, and at chr19q13.12 (in *PROSER3*) with ODI in the medial lemniscus (ML). In sensitivity analyses adding a head motion parameter as a covariate, associations were substantially unchanged (Fig. S3).

Sex-stratified results were comparable in men and women for the 27 genome-wide significant NODDI associations, with the same directions of effect and overlapping confidence intervals, except for a weaker and non-significant association of the chr5q14.3 locus with global NDI in men than women, with a significant sex-interaction in i-Share (Fig. S4). Most genome-wide significant NODDI loci showed significant associations ($p < 1.19 \times 10^{-3}$) with at least one DTI marker (FA or MD). However, only two NODDI-associated variants at chr5q14.3 also showed genome-wide significant association with FA (global measure) and MD (global measure, and in PCR, PTR, SLF, and SS, Figure S5).

### Clinical and molecular correlates of NODDI-associated variants in young adults
We explored associations of genome-wide significant and replicated NODDI susceptibility loci identified in young adults with neurological and vascular traits, using the largest published GWAS for the latter (Table S2). Alleles associated with lower NDI were associated with larger WMH volume at chr5q14.3 (*VCAN*) and
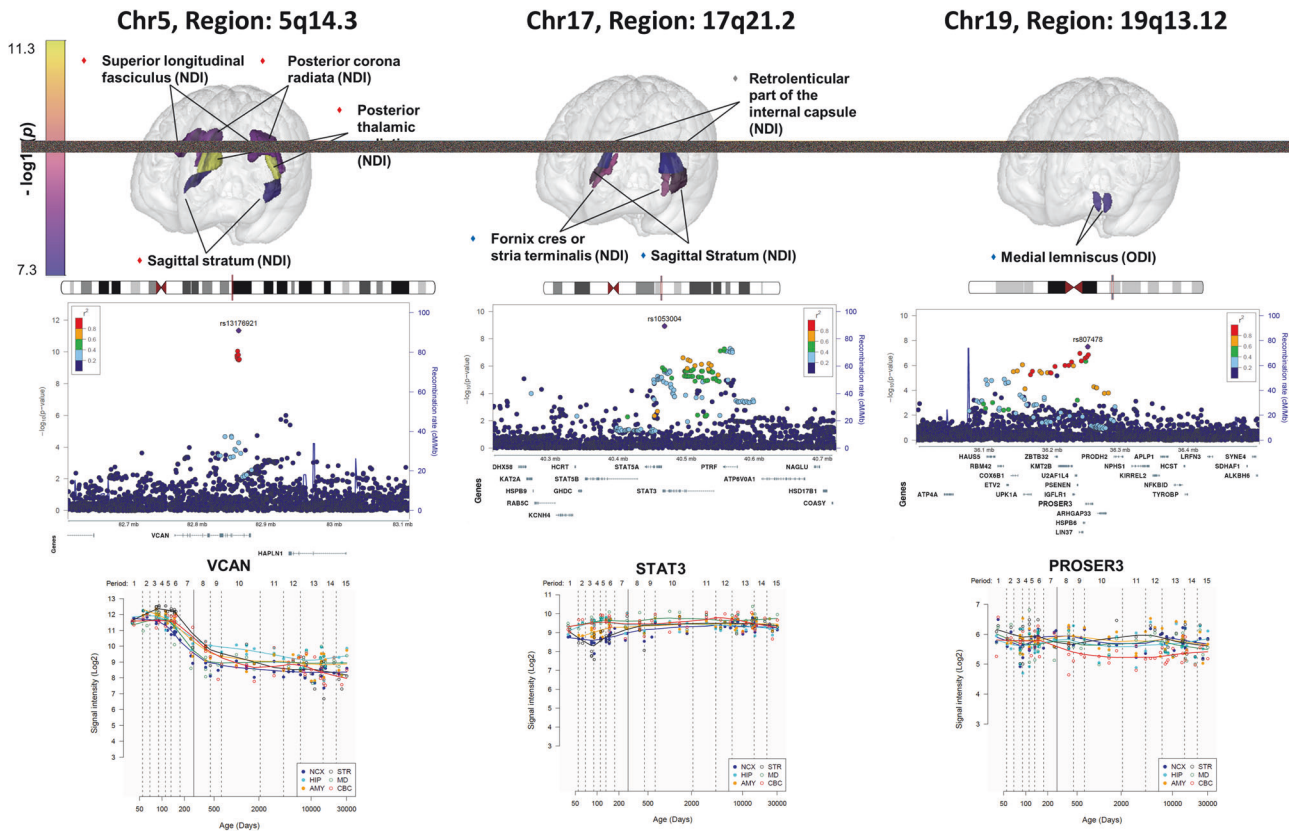
**Fig. 2 Representation of brain regions showing associations with the replicated loci in NODDI marker GWAS with regional plots and lifetime brain gene expression profile of the nearest genes.** The first line shows the localization of the 3 regions with significant and replicated signals in GWAS: chr5q14.3, chr17q21.2 and chr19q13.12. Colors of bullet points on brain projection represent the replication of the loci: red if replicated in all studies, blue for i-Share and UK Biobank, and gray for i-Share only. The second line represents the localization of each locus on the chromosome, combined with a regional plot of the locus. The third line represents the spatio-temporal gene expression level for the nearest gene in each locus (*VCAN*, *STAT3* and *PROSER3* respectively). It is plotted as log2-transformed exon array signal intensity (y-axis) against the post conception days (x-axis) as provided by the Human Brain Transcriptome project database. Periods of human development and adulthood are indicated by vertical dashed lines: 4–8 post conception weeks [PCW] (period 1), 8–10 PCW (period 2), 10–13 PCW (period 3), 13–16 PCW (period 4), 16–19 PCW (period 5), 19-24 PCW (period 6), 24-38 PCW (period 7), birth- 6 postnatal months (period 8), 6–12 postnatal months (period 9), 1–6 years (period 10), 6–12 years (period 11), 12–20 years (period 12), 20–40 years (period 13), 40–60 years (period 14), and 60 years+ (period 15). The boundary between pre- and postnatal periods is indicated by the solid vertical line. Each colored point represents the expression level of each gene across 16 anatomical brain regions and ages. Brain structure includes 11 neocortical areas (NCX, blue), and 5 subcortical regions: hippocampus (HIP, cyan), amygdala (AMY, orange), striatum (STR, black), mediodorsal nucleus of thalamus (MD, dark green), and cerebellar cortex (CBC, red). NDI Neurite Density Index, ODI Orientation Dispersion Index, ISOVF Isotropic Volume Fraction.

with higher pulse pressure and lower risk of multiple sclerosis (MS) at chr17q21.2 (*STAT3*), all at genome-wide significance.

We also explored associations of the 21 genome-wide significant NODDI loci with cognitive tests in the i-Share study (Table S3). At chr9q34.2 (near *RNU6ATAC*), the allele associated with larger ODI (reflecting that the orientations of the neurites spread out more widely in space) was associated with better performance on the matrices test, capturing reasoning and fluid intelligence. In addition, 6 loci were associated with at least one cognitive test at nominal significance ($p < 0.05$), including the 3 replicated loci: at *VCAN* (borderline at $p = 0.05$) and *STAT3* NDI-lowering alleles were associated with worse performance on processing speed and verbal memory tests; at *PROSER3* ODI-increasing alleles were associated with better performance on a vocabulary test.

Next, to explore putative causal genes and directions of effect, we conducted TWAS on the 7 NODDI markers with replicated genome-wide significant loci using TWAS-Fusion and eQTLs based on RNA sequencing in relevant tissues ("Methods"). We identified 32 genes whose genetically regulated expression was associated with NODDI markers (NDI for 19 genes) at $p < 1 \times 10^{-4}$ with

colocalization of GWAS lead variants and eQTL (COLOC-PP4 > 0.75) in at least one tissue (Fig. 3, Fig. S6, Table S4). Higher expression of *STAT3* (at chr17q21.2 NDI locus) in arteries and adipose tissue was significantly associated with lower NDI. Expression levels of five genes at the chr19q13.12 ODI-ML locus (*PROSER3*, *COX6B1*, *UPK1A*, *ZBTB32*, and *KMT2B*) were significantly associated with ODI-ML in vascular and brain tissues (Fig. 3, Fig. S6, Table S4). Finally, when interrogating the human brain transcriptome atlas from embryonic development to late adulthood [53], expression of transcriptome-wide significant genes was either stable across the full lifespan or increased post-natally, while expression of *VCAN* (chr5q14.3 locus) was considerably higher during the prenatal period (Fig. 2 and Fig. S7).

### Association of cerebral small vessel disease (WMH) risk loci with NODDI markers in young adults

First, we explored individual associations of known genetic risk loci for WMH volume identified in older adults (mean age 65 years) [6] with NODDI markers in young i-Share participants in their twenties. Out of 25 loci, 7 showed nominally significant associations with at least one of the three global NODDI markers
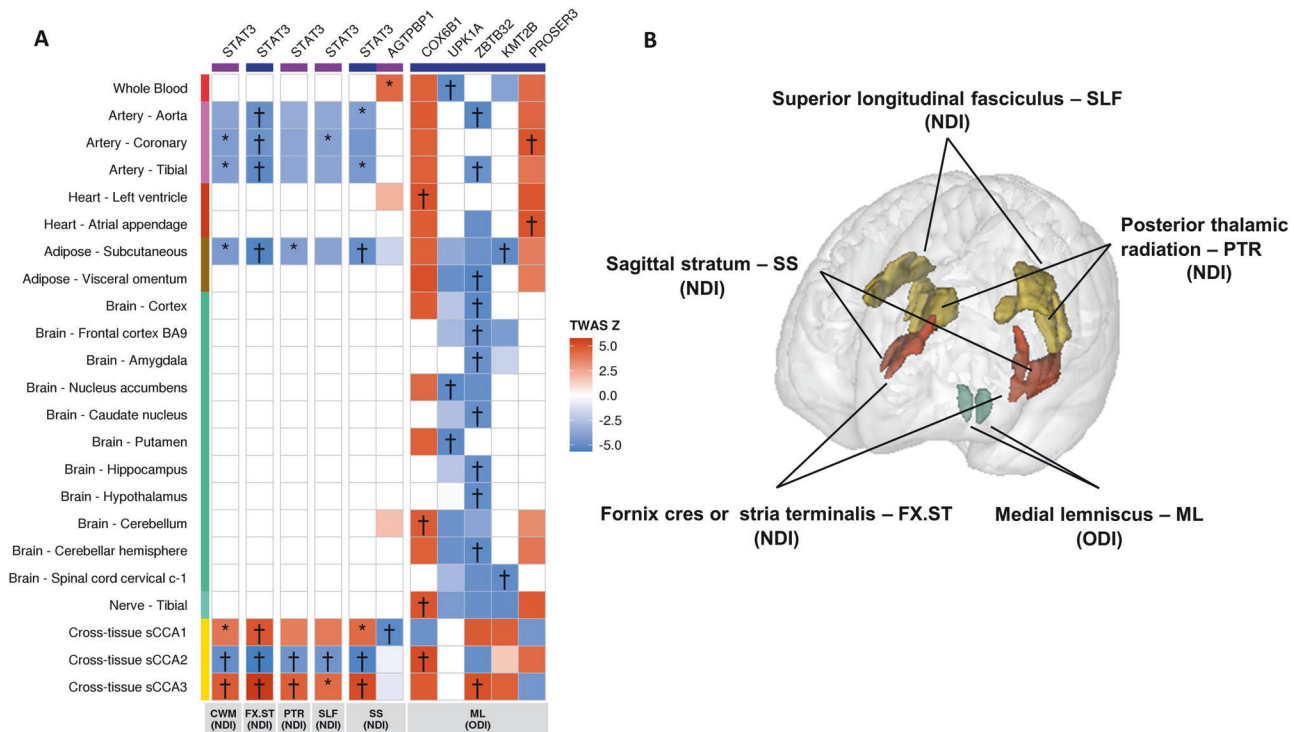
Fig. 3 **Transcriptome-wide association study (TWAS) of NODDI phenotypes in multiple tissues. A** Heatmap of the transcriptome-wide association studies of NODDI markers with genome-wide significant loci in the i-Share study and replicated in the Rhineland study or UK Biobank. Colors in squares represent the association Z-statistic of gene expression with NODDI markers. *: TWAS $p < 1 \times 10^{-4}$, $p < 0.05$ in conditional analyses and COLOC-PP4 > 0.75. † TWAS $p < 7.8 \times 10^{-6}$, $p < 0.05$ in conditional analyses and COLOC-PP4 > 0.75. Only genes with † in at least one tissue for the corresponding phenotype are shown. Genes are presented on the x-axis, those underlined in blue are in a GWAS locus, those underlined in purple are not; Tissue types are on the y-axis (orange: blood; pink: arterial; dark orange: heart; brown: adipose, green: brain; turquoise blue: nerve; gold: cross-tissue weights). sCCA Sparse canonical correlation analysis. **B** Brain representation of regions presenting associations with † in (**A**), with colors representing the types of tissues as on (**A**). NDI Neurite Density Index, ODI Orientation Dispersion Index, ISOVF Isotropic Volume Fraction.

(NDI, ODI, ISOVF). Two of these remained significant after multiple testing correction ($p < 2 \times 10^{-3}$), at chr5q14.3 (*VCAN*) and chr17q21.31 (*NMT1*), the WMH risk allele being associated with lower NDI (Table 2 and Table S5).

Second, we aggregated WMH risk variants in a weighted genetic score to explore their combined association with NODDI markers in young adults. Using both GRS and MR analyses, larger genetically predicted WMH volume was significantly associated with lower NDI, globally and in several regions (Fig. 4, Figs. S8 and S9, Table S6). These associations were found in projection fibers (PCR, PTR, anterior corona radiata (ACR), and superior corona radiata (SCR)) and association fibers (SS and superior longitudinal fasciculus (SLF)). Notably, regions showing associations between genetically predicted WMH and NDI in the young overlapped with regions harboring the highest frequency of WMH in older persons in their seventies (3C-Dijon Study, Fig. 4). Across JHU regions, mean WMH frequency in 3C-Dijon participants correlated significantly with Z-scores of association between the WMH GRS and NDI in i-Share participants (Pearson's $r = -0.54$, $p = 0.0037$, Fig. S10).

Finally, in secondary analyses, as WMH share many genetic risk variants with vascular risk factors, especially blood pressure [6], we explored whether observed associations of NDI with genetically predicted WMH in i-Share merely reflect associations with genetically predicted vascular risk factors (Fig. 4, Figs. S8 and S9, Table S6). Genetically determined high blood pressure and genetic liability to any other vascular risk factor were not associated with NDI in i-Share. The only significant associations observed were between smaller genetically determined BMI and lower regional NDI, in different regions than those associated with genetically

predicted WMH volume (FX.ST and inferior cerebellar peduncle (ICP), Fig. 4).

## DISCUSSION
In this first genomic study of NODDI diffusion markers in young adults, we identified genetic determinants of brain white matter microstructure in early life and shed new light on their relation with cSVD in older age, a leading cause of stroke and dementia worldwide. In total, 21 independent genetic loci were associated with NODDI markers at genome-wide significance. The most prominent and robust signal was at chr5q14.3 (in *VCAN*), a known risk locus for WMH, associated with lower NDI in the whole brain and in 4 regions involving projection and association fibers. These associations were replicated across the adult lifespan, in young middle-aged adults from the Rhineland Study and older adults from UK Biobank. Additional genome-wide significant NODDI loci were replicated in UK Biobank, for NDI markers at chr17q21.2 (*STAT3*), a known pulse pressure and MS locus, and for ODI markers at chr19q13.12 (*PROSER3*). Interestingly, these three main loci were nominally associated with cognitive performance in young adults. Using TWAS, we identified 32 genes of which the genetically determined expression in vascular or brain tissues was associated with NODDI metrics, with evidence for colocalization: 19 with NDI (including *STAT3* at chr17q21.2) and 13 with ODI (including *PROSER3*, *COX6B1*, *UPK1A*, *ZBTB32*, and *KMT2B* at chr19q13.12). Among known WMH risk loci previously identified in older adults, besides chr5q14.3 (*VCAN*), the chr17q21.31 (*NMT1*) locus was associated with lower NDI. Genetically predicted larger WMH volume was significantly associated with lower NDI at age

**Table 2.** Association of known WMH risk variants and global NODDI markers in young adults (i-Share study, n = 1 758).

| SNP | Locus | Pos | Nearest gene | A1 | A0 | FreqA1 | NDI | | ODI | | ISOVF | |
|---|---|---|---|---|---|---|---|---|---|---|---|---|
| | | | | | | | Z | p | Z | p | Z | p |
| Genetic risk score (23 SNPs) | | | | | | | −3.83 | 1.28E-04[a] | 1.09 | 2.76E-01 | 0.99 | 3.22E-01 |
| rs73923006 | 2p21 | 43132224 | *HAAO* | G | C | 0.82 | −0.01 | 9.95E-01 | **2.10** | **3.59E-02** | 1.61 | 1.08E-01 |
| rs17205972 | 5q14.3 | 82859065 | *VCAN* | T | G | 0.19 | **−5.68** | 1.32E-08[a] | 0.02 | 9.81E-01 | **2.46** | **1.38E-02** |
| rs71471298 | 10q24.33 | 105507145 | *SH3PXD2A-AS1* | T | C | 0.11 | **−2.61** | 9.18E-03 | 0.11 | 9.16E-01 | 0.43 | 6.70E-01 |
| rs10786772 | 10q24.33 | 105610326 | *SH3PXD2A* | G | A | 0.69 | −1.68 | 9.25E-02 | 0.44 | 6.61E-01 | **2.40** | **1.64E-02** |
| rs55940034 | 13q34 | 111043309 | *COL4A2* | G | A | 0.31 | **2.14** | 3.25E-02 | 0.79 | 4.30E-01 | −0.66 | 5.07E-01 |
| rs1948948 | 16q12.1 | 51442679 | *SALL1* | C | T | 0.58 | 0.12 | 9.07E-01 | 0.51 | 6.12E-01 | **−2.67** | **7.59E-03** |
| rs6503417 | 17q21.31 | 43144218 | *NMT1* | C | T | 0.63 | −3.41 | 6.46E-04[a] | −0.41 | 6.81E-01 | **2.00** | **4.56E-02** |

A1: effect allele (aligned with allele increasing WMH risk); A0: non-effect allele; Freq: frequency of A1; Z: Z-score defined as Beta of A1 / Standard error.
Only results at least nominally significant with one of the global NODDI markers are presented.
Nominally significant results are in bold.
*NDI* Neurite Density Index, *ODI* Orientation Dispersion Index, *ISOVF* Isotropic Volume Fraction.
[a]Significant results ($p < 2 \times 10^{-3}$ for SNPs; $p < 1.27 \times 10^{-3}$ for genetic risk score).

20, specifically in regions harboring the highest frequency of WMH in older age. This was not driven by genetically determined vascular risk factors.

To our knowledge, this is one of the first studies exploring genetic associations with cutting-edge NODDI markers in young adults and across the adult lifespan, in three complementary cohorts using similar MRI scanners, state-of-the-art protocols and phenotype definitions.

Individually, the most robust genetic association with NODDI markers (NDI) across the adult lifespan was with common intronic variants at chr5q14.3, also a risk locus for WMH in older age [6]. Of note, these variants showed weaker associations in men than women in i-Share only, possibly reflecting previously reported sex differences in brain white matter microstructure [59], including during development [60]. Lead variants were located in introns of *VCAN*, encoding versican, a chondroitin sulfate proteoglycan with multiple isoforms. In the brain *VCAN* is expressed primarily in oligodendrocytes and oligodendrocyte precursor cells, fibroblasts (perivascular and meningeal), and to a lesser extent arterial endothelial cells and arteriolar smooth muscle cells [61–63]. Versican is a major component of the extracellular matrix (ECM), playing a key role in tissue morphogenesis and in regulating immunity and inflammation [64]. Along with *COL4A1*, *COL4A2*, *FGA*, and *MMP12, VCAN* is a main hub in the ECM network across the cerebrovascular matrisome [65], which was recently proposed as a converging pathway in monogenic and multifactorial cSVD [9, 65–68]. Recently, versican was also found to be involved in remyelination in MS, with versican isoform V1 inhibiting remyelination by promoting local T helper 17 cytotoxic neuroinflammation, and versican inhibitors were suggested as a potential dual repair and immunomodulatory therapy for MS [69]. *VCAN* expression in adult vascular and brain bulk tissues was not significantly associated with NODDI markers using TWAS. This could be explained by developmental mechanisms underlying observed genetic associations, *VCAN* expression in the brain being highest in early developmental (prenatal) stages (Fig. 2, Fig. S7), or by cell-type specific, or isoform-specific effects [70]. Interestingly however, in UK Biobank, risk alleles for lower NDI were significantly associated with lower plasma versican protein levels ($p = 8.5 \times 10^{-25}$) measured on the Olink platform [71]. Further explorations, such as single-nuclei isoform RNA sequencing [72], will be required to decipher VCAN isoforms and cell types involved in modulating cSVD risk, to guide experimental follow-up towards potential therapeutic development.

At the second most significant NODDI locus (chr17q21.2) identified in young adults and replicated in older adults, common variants in *STAT3* were associated with NDI in several regions. Higher genetically determined *STAT3* expression in adipose and arterial tissues was associated with lower NDI. Signal transducer and activator of transcription 3 (*STAT3*), encodes a transcription factor expressed in neurons, endothelial cells, astrocytes and microglia [73], activated in response to cytokines and growth factors. *STAT3* plays a key role in neuron and glial cell development, maintenance and survival [74]. The allele associated with lower NDI is known to be associated with higher pulse pressure and lower risk of MS [43, 48]. *STAT3* signaling in myeloid cells promotes pathogenic myelin-specific T-cell differentiation and autoimmune demyelination and was suggested as a therapeutic target for MS [75, 76]. *STAT3* is also involved in the pathogenesis of amyloid deposits in cerebral amyloid angiopathy (a type of cSVD) and Alzheimer's disease [77]. *STAT3*-specific inhibition in a mouse model of amyloidosis improved cognitive function, functional connectivity and increased cerebral blood flow [77]. Inhibition of *STAT3* was also shown to reduce neonatal hypoxic-ischemic brain damage [73].

Intriguingly, both *VCAN* and *STAT3* encode proteins involved in the demyelination/remyelination process in MS. Several epidemiological observations suggest that vascular risk factors and
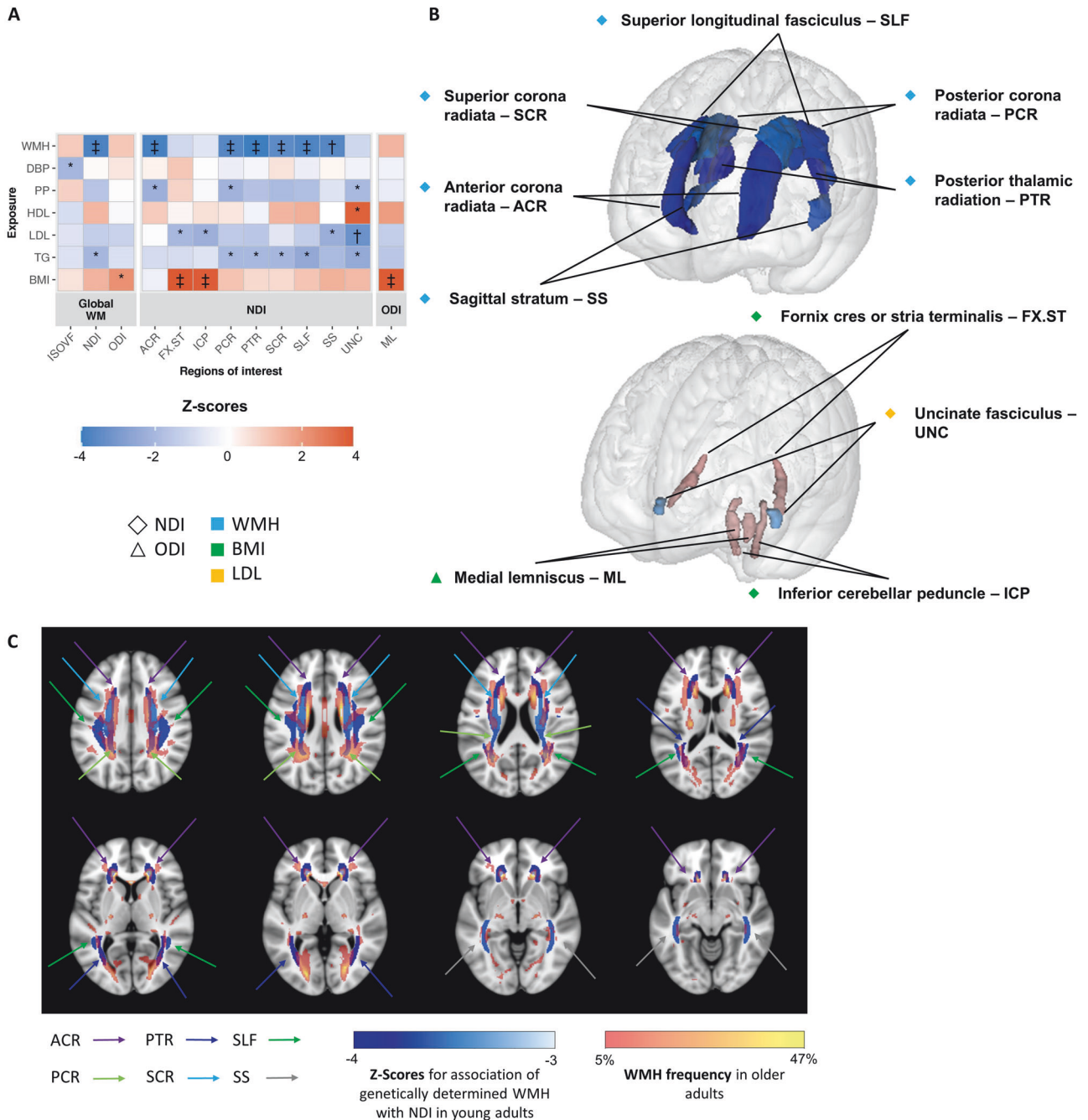
**Fig. 4 Association of genetically-predicted neurovascular traits and vascular risk factors with NODDI metrics in young adults. A** Heatmap of the association of neurovascular traits and vascular risk factors with NODDI metrics in young adults using genetic risk score and Mendelian randomization approaches. Only regions of interest with $p < 1.27 \times 10^{-3}$ in GRS analyses and $p < 0.05$ with at least one method between RadialMR IVW (after removing outliers) and GSMR are shown. Only exposures with $p < 0.05$ in GRS analyses in at least one region of interest are shown. Z-scores correspond to the effect of the GRS of the exposures on the NODDI phenotypes. *$p < 0.05$ with GRS. †$p < 1.27 \times 10^{-3}$ with GRS and $p < 0.05$ with at least one method between RadialMR IVW (after removing outliers) and GSMR. ‡$p < 1.27 \times 10^{-3}$ with GRS and $p < 0.05$ with both RadialMR IVW and GSMR. **B** Projection of significant results on the brain map. Only significant results († or ‡ on **A**) are projected on the brain map. For both **A** and **B**, colors depend on the Z-score values. **C** Overlap with brain regions mostly affected by WMH in older age. The same significant regions for NDI results shown on (**B**), on axial multi-slices to show the overlap with regions affected by WMH in older age; blue scale: Z-score values corresponding to the effect of the GRS for WMH on NDI metrics in young adults (i-Share study); pink to yellow scale: frequency of WMH occurrence in older adults in their seventies (3C). ISOVF Isotropic Volume Fraction, NDI Neurite Density Index, ODI Orientation Dispersion Index, WM White matter, WMH White matter hyperintensities, DBP diastolic blood pressure, PP pulse pressure, HDL HDL-cholesterol, LDL LDL-cholesterol, TG triglycerides, BMI body mass index.

cSVD may contribute to MS severity [78]. Moreover, cSVD and MS share some pathological features, such as white matter demyelination and brain atrophy [78, 79]. Genetic studies have failed to identify shared genetic variation between MS and cSVD, however they were conducted in older populations, with smaller cSVD GWAS datasets than currently available [80]. Our findings suggest that early variations in brain white matter microstructure known to precede cSVD occurrence could perhaps share some biological

pathways with susceptibility to MS, possibly by modulating resilience to brain white matter damage, or via maturational differences in axonal density or degree of myelination [81].

The third genome-wide significant locus for NODDI (ODI in medial lemniscus) in young adults and replicated in older persons, at chr19q13.12, was previously found to be associated with DTI markers of white matter microstructure in UK Biobank [22, 82]. At this locus, TWAS identified associations of NODDI markers with genetically determined expression levels of several genes (*PROSER3*, *COX6B1*, *UPK1A*, *ZBTB32* and *KMT2B*), all with significant colocalization and in different brain and vascular tissues. Two of these genes, *COX6B1* and *KMT2B*, are involved in monogenic childhood-onset neurological disorders with cognitive decline and delayed motor or cognitive development [83–86]. Interestingly, several transcriptome-wide significant and colocalized genes outside genome-wide significant GWAS loci point to biologically relevant pathways related to neurodevelopment and neurodegeneration (*PICALM*, a known Alzheimer disease gene [47, 87–89], *CAMSAP2*, *AGTPBP1*, *SETD1A*, *EPRS*, *PADI2* and *PSAP*).

Our results support a robust relation between genetic determinants of WMH, the most common imaging feature of cSVD in older adults, and NODDI markers, especially NDI, in young adults. Interestingly, associations of genetically predicted WMH with NDI markers at age 20 were observed primarily in white matter regions most commonly affected by WMH in older age [90, 91], such as the anterior, posterior and superior corona radiata, posterior thalamic radiation, and superior longitudinal fasciculus. This corroborates recent observations that areas where WMH are most likely to appear in older adults are also those with the lowest white matter microstructure integrity on DTI in young adults [91]. In contrast, we found no association of genetically determined blood pressure, the main known risk factor for WMH, with NDI, suggesting that the association between genetically predicted WMH and NDI was likely not mediated by blood pressure. Our results could suggest that NDI, although not specific may be particularly sensitive to variations in the white matter microstructure reflecting a higher propensity to develop WMH, already detectable early in life [17]. Of note, we recently showed significant decrease in NDI values in WMH lesions compared to normal appearing white matter in i-Share participants [88], supporting that NDI is sensitive to microstructural alterations related to WMH. NDI represents the density of neurites relative to extra-neurite volume. Thus, besides neurite density itself, it could also be influenced by changes in components of the extra-neurite volume, e.g. extracellular matrix, known to play a central role in cSVD [9].

Individually, two known WMH risk loci were associated with global NODDI markers after multiple testing correction, in *VCAN* and *NMT1*. While these loci were previously associated with DTI markers in young adults [6], our results provide novel insights into tissue-based mechanisms, showing associations specifically with lower NDI. Additional WMH risk loci were associated with NODDI markers at *P* < 0.05, with NDI and ISOVF at the *SH3PXD2A* locus, previously associated with DTI markers [6], with ISOVF at the *SALL1* locus (a microglial signature gene) [92], and with NDI at the *COL4A1* locus (a gene harboring rare mutations causing monogenic cSVD) [93].

We acknowledge limitations. We did not apply any data harmonization approach to the imaging datasets [94], as we did not combine them; this will be important to consider for future meta-analyses of NODDI GWAS to enhance power for detecting novel associations. NODDI makes certain assumptions that can bias the estimates when they are not met [95, 96]. It assumes a fixed diffusivity for both intra- and extracellular spaces that can cause non-negligible biases in ODI and ISOVF [95]. However, it is one of the few tissue-based models that have been extensively validated histologically [97–99]. Moreover, in secondary analyses we showed that most of the genome-wide significant associations identified with NODDI markers would not have been identified using the standard DTI metrics. Thus, by providing more biologically specific estimates that disambiguate contributions of fiber packing, orientations, and CSF contamination on the diffusion signal, NODDI may offer more sensitive measures of microstructural properties relevant for susceptibility to cSVD than DTI. The cohort of young adults, although unique, was of limited sample size. Further studies in other young cohorts, including in even younger individuals, will be crucial to strengthen our findings and expand them further across the lifespan. The fact that associations of genetic variants for WMH with NODDI metrics in young adults clustered in regions that also harbor the highest frequency of WMH in older age only indirectly supports that NODDI changes may precede WMH in these regions. Ideally, this should be confirmed in the future through a longitudinal design across the lifespan (to our knowledge repeated MRIs in the same individuals from young to older adulthood are currently not available). To explore the relation of NODDI markers with genetically predicted cSVD we used genetic instruments for total WMH volume. In the future, when well powered GWAS of WMH spatial patterns become available, they may allow to better account for the heterogeneity of pathological mechanisms underlying cSVD and provide more granular insights into its lifespan determinants. We cannot exclude bias from postmortem changes in TWAS and analyses of lifetime brain gene expression, as available tissues were mostly from deceased persons [100]. Finally, we used cohorts of predominantly European ancestry and enriched in participants from privileged regions of the world, thus limiting the generalizability of our results. Over 95% of participants in genetic studies on brain MRI traits are of European ancestry and efforts to enhance diversity in this context are of paramount importance [13].

In summary, our study identified novel genetic determinants of NODDI markers of white matter microstructure in young adults. Leveraging this and other resources it provides important novel insights into early-life determinants of cSVD, a leading cause of stroke and dementia. Genetically predicted cSVD burden appears associated with lower neurite density index already at age 20, specifically in regions most likely to harbor cSVD lesions in later life. Genome-wide significant associations with NODDI markers in early adulthood point to genes related to neurodevelopmental, neurodegenerative, and neuroinflammatory processes. Further research is warranted to decipher the molecular pathways and mechanisms involved, as this could open avenues for entirely novel approaches to early prevention.

## DATA AVAILABILITY

## CODE AVAILABILITY

## REFERENCES

1. Alber J, Alladi S, Bae H-J, Barton DA, Beckett LA, Bell JM, et al. White matter hyperintensities in vascular contributions to cognitive impairment and dementia (VCID): Knowledge gaps and opportunities. Alzheimers Dement Transl Res Clin Interv. 2019;5:107–17.
2. Pasi M, Cordonnier C. Clinical relevance of cerebral small vessel diseases. Stroke. 2020;51:47–53.
3. Chauhan G, Adams HHH, Satizabal CL, Bis JC, Teumer A, Sargurupremraj M, et al. Genetic and lifestyle risk factors for MRI-defined brain infarcts in a population-based setting. Neurology. 2019;92:e486–e503. https://doi.org/10.1212/WNL.0000000000006851
4. Debette S, Schilling S, Duperron M-G, Larsson SC, Markus HS. Clinical significance of magnetic resonance imaging markers of vascular brain injury: a systematic review and meta-analysis. JAMA Neurol. 2019;76:81–94.
5. Mishra A, Chauhan G, Violleau M-H, Vojinovic D, Jian X, Bis JC, et al. Association of variants in HTRA1 and NOTCH3 with MRI-defined extremes of cerebral small vessel disease in older subjects. Brain. 2019;142:1009–23.
6. Sargurupremraj M, Suzuki H, Jian X, Sarnowski C, Evans TE, Bis JC, et al. Cerebral small vessel disease genomics and its implications across the lifespan. Nat Commun. 2020;11:6285.
7. Sargurupremraj M., Soumare A., Bis J. C., Surakka I., Jurgenson T., Joly P., et al. Complexities of cerebral small vessel disease, blood pressure, and dementia relationship: new insights from genetics. MedRxiv Prepr Serv Health Sci. 2023:2023.08.08.23293761.
8. Wardlaw JM, Debette S, Jokinen H, De Leeuw F-E, Pantoni L, Chabriat H, et al. ESO Guideline on covert cerebral small vessel disease. Eur Stroke J. 2021;6:CXI–CLXII.
9. Bordes C, Sargurupremraj M, Mishra A, Debette S. Genetics of common cerebral small vessel disease. Nat Rev Neurol. 2022;18:84–101.
10. Persyn E, Hanscombe KB, Howson JMM, Lewis CM, Traylor M, Markus HS. Genome-wide association study of MRI markers of cerebral small vessel disease in 42,310 participants. Nat Commun. 2020;11:2175.
11. Baykara E, Gesierich B, Adam R, Tuladhar AM, Biesbroek JM, Koek HL, et al. A novel imaging marker for small vessel disease based on skeletonization of white matter tracts and diffusion histograms. Ann Neurol. 2016;80:581–92.
12. Tuladhar AM, van Norden AGW, de Laat KF, Zwiers MP, van Dijk EJ, Norris DG, et al. White matter integrity in small vessel disease is related to cognition. NeuroImage Clin. 2015;7:518–24.
13. Duperron M-G, Knol MJ, Le Grand Q, Evans TE, Mishra A, Tsuchida A, et al. Genomics of perivascular space burden unravels early mechanisms of cerebral small vessel disease. Nat Med. 2023;29:950–62.
14. Backhouse EV, Shenkin SD, McIntosh AM, Bastin ME, Whalley HC, Valdez Hernandez M, et al. Early life predictors of late life cerebral small vessel disease in four prospective cohort studies. Brain J Neurol. 2021;144:3769–78.
15. Barnat M, Capizzi M, Aparicio E, Boluda S, Wennagel D, Kacher R, et al. Huntington's disease alters human neurodevelopment. Science. 2020;369:787–93.
16. Braz BY, Wennagel D, Ratié L, de Souza DAR, Deloulme JC, Barbier EL, et al. Treating early postnatal circuit defect delays Huntington's disease onset and pathology in mice. Science. 2022;377:eabq5011.
17. Kamiya K, Hori M, Aoki S. NODDI in clinical research. J Neurosci Methods. 2020;346:108908.
18. Jones DK, Knösche TR, Turner R. White matter integrity, fiber count, and other fallacies: the do's and don'ts of diffusion MRI. NeuroImage. 2013;73:239–54.
19. Tsuchida A, Laurent A, Crivello F, Petit L, Pepe A, Beguedou N, et al. Age-related variations in regional white matter volumetry and microstructure during the post-adolescence period: a cross-sectional study of a cohort of 1713 university students. Front Syst Neurosci. 2021;15:692152.
20. Zhang H, Schneider T, Wheeler-Kingshott CA, Alexander DC. NODDI: practical in vivo neurite orientation dispersion and density imaging of the human brain. NeuroImage. 2012;61:1000–16.
21. Motovylyak A, Vogt NM, Adluru N, Ma Y, Wang R, Oh JM, et al. Age-related differences in white matter microstructure measured by advanced diffusion MRI in healthy older adults at risk for Alzheimer's disease. Aging Brain. 2022;2:100030.
22. Smith SM, Douaud G, Chen W, Hanayik T, Alfaro-Almagro F, Sharp K, et al. An expanded set of genome-wide association studies of brain imaging phenotypes in UK Biobank. Nat Neurosci. 2021;24:737–45.
23. Montagni I, Guichard E, Kurth T. Association of screen time with self-perceived attention problems and hyperactivity levels in French students: a cross-sectional study. BMJ Open. 2016;6:e009089.
24. Tsuchida A, Laurent A, Crivello F, Petit L, Joliot M, Pepe A, et al. The MRi-Share database: brain imaging in a cross-sectional cohort of 1870 university students. Brain Struct Funct. 2021;226:2057–85.
25. Le Grand Q, Satizabal CL, Sargurupremraj M, Mishra A, Soumaré A, Laurent A, et al. Genomic studies across the lifespan point to early mechanisms determining subcortical volumes. Biol Psychiatry Cogn Neurosci Neuroimaging. 2022;7:616–28.
26. Lohner V, Enkirch SJ, Hattingen E, Stöcker T, Breteler MMB. Safety of tattoos, permanent make-up, and medical implants in population-based 3T magnetic resonance brain imaging: the Rhineland Study. Front Neurol. 2022;13:795573.
27. Miller KL, Alfaro-Almagro F, Bangerter NK, Thomas DL, Yacoub E, Xu J, et al. Multimodal population brain imaging in the UK Biobank prospective epidemiological study. Nat Neurosci. 2016;19:1523–36.
28. Alfaro-Almagro F, Jenkinson M, Bangerter NK, Andersson JLR, Griffanti L, Douaud G, et al. Image processing and Quality Control for the first 10,000 brain imaging datasets from UK Biobank. NeuroImage. 2018;166:400–24.
29. Tobisch A, Stirnberg R, Harms RL, Schultz T, Roebroeck A, Breteler MMB, et al. Compressed sensing diffusion spectrum imaging for accelerated diffusion microstructure MRI in long-term population imaging. Front Neurosci. 2018;12:650.
30. Fischl B, Salat DH, Busa E, Albert M, Dieterich M, Haselgrove C, et al. Whole Brain Segmentation. Neuron. 2002;33:341–55.
31. Fischl B. FreeSurfer. NeuroImage. 2012;62:774–81.
32. Andersson JLR, Skare S, Ashburner J. How to correct susceptibility distortions in spin-echo echo-planar images: application to diffusion tensor imaging. NeuroImage. 2003;20:870–88.
33. Tobisch A, Schultz T, Stirnberg R, Varela-Mattatall G, Knutsson H, Irarrázaval P, et al. Comparison of basis functions and q-space sampling schemes for robust compressed sensing reconstruction accelerating diffusion spectrum imaging. NMR Biomed. 2019;32:e4055.
34. Basser PJ, Mattiello J, LeBihan D. MR diffusion tensor spectroscopy and imaging. Biophys J. 1994;66:259–67.
35. Harms RL, Fritz FJ, Tobisch A, Goebel R, Roebroeck A. Robust and fast nonlinear optimization of diffusion MRI microstructure models. NeuroImage. 2017;155:82–96.
36. Smith SM, Jenkinson M, Johansen-Berg H, Rueckert D, Nichols TE, Mackay CE, et al. Tract-based spatial statistics: voxelwise analysis of multi-subject diffusion data. NeuroImage. 2006;31:1487–505.
37. Mori S, Oishi K, Jiang H, Jiang L, Li X, Akhter K, et al. Stereotaxic white matter atlas based on diffusion tensor imaging in an ICBM template. NeuroImage. 2008;40:570–82.
38. Coors A, Imtiaz M-A, Boenniger MM, Aziz NA, Ettinger U, Breteler MMB. Associations of genetic liability for Alzheimer's disease with cognition and eye movements in a large, population-based cohort study. Transl Psychiatry. 2022;12:337.
39. Bycroft C, Freeman C, Petkova D, Band G, Elliott LT, Sharp K, et al. The UK Biobank resource with deep phenotyping and genomic data. Nature. 2018;562:203–9.
40. Mbatchou J, Barnard L, Backman J, Marcketta A, Kosmicki JA, Ziyatdinov A, et al. Computationally efficient whole-genome regression for quantitative and binary traits. Nat Genet. 2021;53:1097–103.
41. Li J, Ji L. Adjusting multiple testing in multilocus analyses using the eigenvalues of a correlation matrix. Heredity. 2005;95:221–7.
42. Liu D, Aziz NA, Imtiaz MA, Pehlivan G, Breteler MMB. Associations of measured and genetically predicted leukocyte telomere length with vascular phenotypes: a population-based study. GeroScience. 2024;46:1947–70.
43. Evangelou E, Warren HR, Mosen-Ansorena D, Mifsud B, Pazoki R, Gao H, et al. Genetic analysis of over one million people identifies 535 new loci associated with blood pressure traits. Nat Genet. 2018;50:1412–25.
44. Graham SE, Clarke SL, Wu K-HH, Kanoni S, Zajac GJM, Ramdas S, et al. The power of genetic diversity in genome-wide association studies of lipids. Nature. 2021;600:675–9.
45. Pulit SL, Stoneman C, Morris AP, Wood AR, Glastonbury CA, Tyrrell J, et al. Meta-analysis of genome-wide association studies for body fat distribution in 694 649 individuals of European ancestry. Hum Mol Genet. 2019;28:166–74.
46. Mahajan A, Taliun D, Thurner M, Robertson NR, Torres JM, Rayner NW, et al. Fine-mapping type 2 diabetes loci to single-variant resolution using high-density imputation and islet-specific epigenome maps. Nat Genet. 2018;50:1505–13.
47. Bellenguez C, Küçükali F, Jansen IE, Kleineidam L, Moreno-Grau S, Amin N, et al. New insights into the genetic etiology of Alzheimer's disease and related dementias. Nat Genet. 2022;54:412–36.
48. International Multiple Sclerosis Genetics Consortium. Multiple sclerosis genomic map implicates peripheral immune cells and microglia in susceptibility. Science. 2019;365:eaav7188.
49. Gusev A, Ko A, Shi H, Bhatia G, Chung W, Penninx BWJH, et al. Integrative approaches for large-scale transcriptome-wide association studies. Nat Genet. 2016;48:245–52.

50. GTEx Consortium. The GTEx Consortium atlas of genetic regulatory effects across human tissues. Science. 2020;369:1318–30.

51. Feng H, Mancuso N, Gusev A, Majumdar A, Major M, Pasaniuc B, et al. Leveraging expression from multiple tissues using sparse canonical correlation analysis and aggregate tests improves the power of transcriptome-wide association studies. PLoS Genet. 2021;17:e1008973.

52. Giambartolomei C, Vukcevic D, Schadt EE, Franke L, Hingorani AD, Wallace C, et al. Bayesian test for colocalisation between pairs of genetic association studies using summary statistics. PLoS Genet. 2014;10:e1004383.

53. Kang HJ, Kawasawa YI, Cheng F, Zhu Y, Xu X, Li M, et al. Spatio-temporal transcriptome of the human brain. Nature. 2011;478:483–9.

54. Bowden J, Spiller W, Del Greco M F, Sheehan N, Thompson J, Minelli C, et al. Improving the visualization, interpretation and analysis of two-sample summary data Mendelian randomization via the Radial plot and Radial regression. Int J Epidemiol. 2018;47:1264–78.

55. Zhu Z, Zheng Z, Zhang F, Wu Y, Trzaskowski M, Maier R, et al. Causal associations between risk factors and common diseases inferred from GWAS summary data. Nat Commun. 2018;9:224.

56. Hemani G, Zheng J, Elsworth B, Wade KH, Haberland V, Baird D, et al. The MR-Base platform supports systematic causal inference across the human phenome. eLife. 2018;7:e34408.

57. Maillard P, Delcroix N, Crivello F, Dufouil C, Gicquel S, Joliot M, et al. An automated procedure for the assessment of white matter hyperintensities by multispectral (T1, T2, PD) MRI and an evaluation of its between-centre reproducibility based on two large community databases. Neuroradiology. 2008;50:31–42.

58. 3C Study Group. Vascular factors and risk of dementia: design of the three-city study and baseline characteristics of the study population. Neuroepidemiology. 2003;22:316–25.

59. Lawrence KE, Nabulsi L, Santhalingam V, Abaryan Z, Villalon-Reina JE, Nir TM, et al. Age and sex effects on advanced white matter microstructure measures in 15,628 older adults: a UK biobank study. Brain Imaging Behav. 2021;15:2813–23.

60. Benavidez S. M., Abaryan Z., Kim G. S., Laltoo E., McCracken J. T., Thompson P. M., et al. Sex differences in the brain's white matter microstructure during development assessed using advanced diffusion MRI models. BioRxiv Prepr Serv Biol. 2024:2024.02.02.578712.

61. He L, Vanlandewijck M, Mäe MA, Andrae J, Ando K, Del Gaudio F, et al. Single-cell RNA sequencing of mouse brain and lung vascular and vessel-associated cell types. Sci Data. 2018;5:180160.

62. Vanlandewijck M, He L, Mäe MA, Andrae J, Ando K, Del Gaudio F, et al. A molecular atlas of cell types and zonation in the brain vasculature. Nature. 2018;554:475–80.

63. Yang AC, Vest RT, Kern F, Lee DP, Agam M, Maat CA, et al. A human brain vascular atlas reveals diverse mediators of Alzheimer's risk. Nature. 2022;603:885–92.

64. Wight TN, Kang I, Evanko SP, Harten IA, Chang MY, Pearce OMT, et al. Versican-a critical extracellular matrix regulator of immunity and inflammation. Front Immunol. 2020;11:512.

65. Pokhilko A, Brezzo G, Handunnetthi L, Heilig R, Lennon R, Smith C, et al. Global proteomic analysis of extracellular matrix in mouse and human brain highlights relevance to cerebrovascular disease. J Cereb Blood Flow Metab. 2021;41:2423–38.

66. Rosenberg GA. Extracellular matrix inflammation in vascular cognitive impairment and dementia. Clin Sci Lond Engl. 2017;131:425–37.

67. Joutel A, Haddad I, Ratelade J, Nelson MT. Perturbations of the cerebrovascular matrisome: A convergent mechanism in small vessel disease of the brain? J Cereb Blood Flow Metab Off J Int Soc Cereb Blood Flow Metab. 2016;36:143–57.

68. Tan R, Traylor M, Rutten-Jacobs L, Markus H. New insights into mechanisms of small vessel disease stroke from genetics. Clin Sci Lond Engl. 2017;131:515–31.

69. Ghorbani S, Jelinek E, Jain R, Buehner B, Li C, Lozinski BM, et al. Versican promotes T helper 17 cytotoxic inflammation and impedes oligodendrocyte precursor cell remyelination. Nat Commun. 2022;13:2445.

70. Zheng P-S, Wen J, Ang LC, Sheng W, Viloria-Petit A, Wang Y, et al. Versican/PG-M G3 domain promotes tumor growth and angiogenesis. FASEB J. 2004;18:754–6.

71. Sun BB, Chiou J, Traylor M, Benner C, Hsu Y-H, Richardson TG, et al. Plasma proteomic associations with genetics and health in the UK Biobank. Nature. 2023;622:329–38.

72. Hardwick SA, Hu W, Joglekar A, Fan L, Collier PG, Foord C, et al. Single-nuclei isoform RNA sequencing unlocks barcoded exon connectivity in frozen brain tissue. Nat Biotechnol. 2022;40:1082–92.

73. Hristova M, Rocha-Ferreira E, Fontana X, Thei L, Buckle R, Christou M, et al. Inhibition of Signal Transducer and Activator of Transcription 3 (STAT3) reduces neonatal hypoxic-ischaemic brain damage. J Neurochem. 2016;136:981–94.

74. Dziennis S, Alkayed NJ. Role of signal transducer and activator of transcription 3 in neuronal survival and regeneration. Rev Neurosci. 2008;19:341–61.

75. Steelman AJ, Zhou Y, Koit H, Kim S, Payne HR, Lu QR, et al. Activation of oligodendroglial Stat3 is required for efficient remyelination. Neurobiol Dis. 2016;91:336–46.

76. Lu HC, Kim S, Steelman AJ, Tracy K, Zhou B, Michaud D, et al. STAT3 signaling in myeloid cells promotes pathogenic myelin-specific T cell differentiation and autoimmune demyelination. Proc Natl Acad Sci USA. 2020;117:5430–41.

77. Mehla J, Singh I, Diwan D, Nelson JW, Lawrence M, Lee E, et al. STAT3 inhibitor mitigates cerebral amyloid angiopathy and parenchymal amyloid plaques while improving cognitive functions and brain networks. Acta Neuropathol Commun. 2021;9:193.

78. Geraldes R, Esiri MM, DeLuca GC, Palace J. Age-related small vessel disease: a potential contributor to neurodegeneration in multiple sclerosis. Brain Pathol Zurich Switz. 2017;27:707–22.

79. Wang B, Li X, Li H, Xiao L, Zhou Z, Chen K, et al. Clinical, radiological and pathological characteristics between cerebral small vessel disease and multiple sclerosis: a review. Front Neurol. 2022;13:841521.

80. Brown RB, Traylor M, Burgess S, Sawcer S, Markus HS. Do cerebral small vessel disease and multiple sclerosis share common mechanisms of white matter injury? Stroke. 2019;50:1968–72.

81. Grussu F, Schneider T, Tur C, Yates RL, Tachrount M, Ianuş A, et al. Neurite dispersion: a new marker of multiple sclerosis spinal cord pathology? Ann Clin Transl Neurol. 2017;4:663–79.

82. Zhao B, Zhang J, Ibrahim JG, Luo T, Santelli RC, Li Y, et al. Large-scale GWAS reveals genetic architecture of brain white matter microstructure and genetic overlap with cognitive and mental health traits ($n = 17,706$). Mol Psychiatry. 2021;26:3943–55.

83. Abdulhag UN, Soiferman D, Schueler-Furman O, Miller C, Shaag A, Elpeleg O, et al. Mitochondrial complex IV deficiency, caused by mutated COX6B1, is associated with encephalomyopathy, hydrocephalus and cardiomyopathy. Eur J Hum Genet EJHG. 2015;23:159–64.

84. Massa V, Fernandez-Vizarra E, Alshahwan S, Bakhsh E, Goffrini P, Ferrero I, et al. Severe infantile encephalomyopathy caused by a mutation in COX6B1, a nucleus-encoded subunit of cytochrome c oxidase. Am J Hum Genet. 2008;82:1281–9.

85. Zech M, Boesch S, Maier EM, Borggraefe I, Vill K, Laccone F, et al. Haploinsufficiency of KMT2B, encoding the lysine-specific histone methyltransferase 2B, results in early-onset generalized dystonia. Am J Hum Genet. 2016;99:1377–87.

86. Meyer E, Carss KJ, Rankin J, Nichols JME, Grozeva D, Joseph AP, et al. Mutations in the histone methyltransferase gene KMT2B cause complex early-onset dystonia. Nat Genet. 2017;49:223–37.

87. Fyfe I. Alzheimer disease-associated gene increases tau pathology. Nat Rev Neurol. 2020;16:128.

88. Xu W, Tan L, Yu J-T. The role of PICALM in Alzheimer's disease. Mol Neurobiol. 2015;52:399–413.

89. Jun G, Naj AC, Beecham GW, Wang L-S, Buros J, Gallins PJ, et al. Meta-analysis confirms CR1, CLU, and PICALM as Alzheimer disease risk loci and reveals interactions with APOE genotypes. Arch Neurol. 2010;67:1473–84.

90. Habes M, Erus G, Toledo JB, Bryan N, Janowitz D, Doshi J, et al. Regional tract-specific white matter hyperintensities are associated with patterns to aging-related brain atrophy via vascular risk factors, but also independently. Alzheimers Dement 2018;10:278–84.

91. Lao PJ, Vorburger RS, Narkhede A, Gazes Y, Igwe KC, Colón J, et al. White matter regions with low microstructure in young adults spatially coincide with white matter hyperintensities in older adults. Front Aging Neurosci. 2019;11:345.

92. Buttgereit A, Lelios I, Yu X, Vrohlings M, Krakoski NR, Gautier EL, et al. Sall1 is a transcriptional regulator defining microglia identity and function. Nat Immunol. 2016;17:1397–406.

93. Gould DB, Phalan FC, van Mil SE, Sundberg JP, Vahedi K, Massin P, et al. Role of COL4A1 in small-vessel disease and hemorrhagic stroke. N Engl J Med. 2006;354:1489–96.

94. Fortin J-P, Parker D, Tunç B, Watanabe T, Elliott MA, Ruparel K, et al. Harmonization of multi-site diffusion tensor imaging data. NeuroImage. 2017;161:149–70.

95. Jelescu IO, Veraart J, Adisetiyo V, Milla SS, Novikov DS, Fieremans E. One diffusion acquisition and different white matter models: how does microstructure change in human early development based on WMTI and NODDI? NeuroImage. 2015;107:242–56.

96. Lampinen B, Szczepankiewicz F, Mårtensson J, van Westen D, Sundgren PC, Nilsson M. Neurite density imaging versus imaging of microscopic anisotropy in diffusion MRI: A model comparison using spherical tensor encoding. NeuroImage. 2017;147:517–31.

97. Sepehrband F, Clark KA, Ullmann JFP, Kurniawan ND, Leanage G, Reutens DC, et al. Brain tissue compartment density estimated using diffusion-weighted MRI yields tissue parameters consistent with histology. Hum Brain Mapp. 2015;36:3687–702.

98. Sato K, Kerever A, Kamagata K, Tsuruta K, Irie R, Tagawa K, et al. Understanding microstructure of the brain by comparison of neurite orientation dispersion and density imaging (NODDI) with transparent mouse brain. Acta Radiol Open. 2017;6:2058460117703816.

99. Schilling KG, Janve V, Gao Y, Stepniewska I, Landman BA, Anderson AW. Histological validation of diffusion MRI fiber orientation distributions and dispersion. NeuroImage. 2018;165:200–21.

100. Garcia FJ, Sun N, Lee H, Godlewski B, Mathys H, Galani K, et al. Single-cell dissection of the human brain vasculature. Nature. 2022;603:893–9.

## ACKNOWLEDGEMENTS

## AUTHOR CONTRIBUTIONS

## FUNDING

## COMPETING INTERESTS

PMM is a member of the Steering Committee of UK Biobank. The authors report no other competing interests.

## ADDITIONAL INFORMATION

**Supplementary information** The online version contains supplementary material available at https://doi.org/10.1038/s41380-024-02604-7.

**Correspondence** and requests for materials should be addressed to Stéphanie Debette.

**Reprints and permission information** is available at http://www.nature.com/reprints

**Publisher's note** Springer Nature remains neutral with regard to jurisdictional claims in published maps and institutional affiliations.